

Structure Matters: Brain Graph Augmentation via Learnable Edge Masking for Data-efficient Psychiatric Diagnosis

Mujie Liu¹, Chenze Wang², Liping Chen³, Nguyen Linh Dan Le³, Niharika Tewari³, Ting Dang⁴, Jiangang Ma¹, and Feng Xia³  

¹ Institute of Innovation, Science and Sustainability, Federation University Australia, Ballarat 3353, Australia

² School of Information and Electronic Engineering, Zhejiang Gongshang University, Hangzhou 315104, China

³ School of Computing Technologies, RMIT University, Melbourne 3000, Australia

⁴ School of Computing and Information Systems, The University of Melbourne, Melbourne 3052, Australia

mujie.liu@ieee.org, 23020090112@pop.zjgsu.edu.cn, lp.chen@ieee.org, s4135772@student.rmit.edu.au, S4044597@student.rmit.edu.au, ting.dang@unimelb.edu.au, j.ma@federation.edu.au, f.xia@ieee.org

Abstract. The limited availability of labeled brain network data makes it challenging to achieve accurate and interpretable psychiatric diagnoses. While self-supervised learning (SSL) offers a promising solution, existing methods often rely on augmentation strategies that can disrupt crucial structural semantics in brain graphs. To address this, we propose SAM-BG, a two-stage framework for learning brain graph representations with structural semantic preservation. In the pre-training stage, an edge masker is trained on a small labeled subset to capture key structural semantics. In the SSL stage, the extracted structural priors guide a structure-aware augmentation process, enabling the model to learn more semantically meaningful and robust representations. Experiments on two real-world psychiatric datasets demonstrate that SAM-BG outperforms state-of-the-art methods, particularly in small-labeled data settings, and uncovers clinically relevant connectivity patterns that enhance interpretability. Our code is available at <https://github.com/mjliu99/SAM-BG>.

Keywords: Psychiatric Diagnosis · Brain Graph Representation · Self-supervised Learning · Structure Semantics · fMRI · Graph Learning.

1 Introduction

Functional magnetic resonance imaging (fMRI) is a widely adopted neuroimaging technique in neuroscience research. By capturing blood-oxygen-level-dependent (BOLD) signals, fMRI enables functional connectivity measurement, allowing researchers to monitor brain activity and assess neurological development [26].

Increasing evidence shows that disruptions in brain network connectivity are closely linked to the onset and progression of various neurological and psychiatric disorders [10]. These findings underscore the importance of developing advanced computational methods tailored to fMRI data to better support clinical diagnostics and mental health care through physiologically grounded brain network analysis [2].

Graph learning [24] has emerged as a powerful tool in this context, representing fMRI data as brain graphs where nodes correspond to brain regions and edges represent functional connections. Leveraging graph neural networks (GNNs), these methods effectively capture complex connectivity patterns and have shown strong potential in tasks such as disease classification and biomarker discovery [17, 22]. However, their success often depends on large-scale labeled datasets, which are scarce in psychiatric research due to privacy concerns and the high cost of expert annotations. For example, labeling patients with autism spectrum disorder (ASD) typically requires long-term behavioral observation and developmental assessments conducted by trained clinicians [9].

To alleviate this challenge, self-supervised learning (SSL) has emerged as a promising paradigm for learning meaningful representations from unlabeled data [13, 25]. SSL-based methods typically rely on generic graph augmentation strategies such as random edge perturbation, node masking, or subgraph sampling to generate multiple views for contrastive or predictive learning [14, 19, 23, 31]. While effective in general graph domains, these augmentation methods are task-agnostic and domain-independent, often neglecting domain-specific structural priors. In brain network analysis, such priors are particularly crucial, as they encode biologically meaningful structural semantics, often manifested as connectivity patterns (substructures), which are closely associated with psychiatric disorders [7]. Thus, indiscriminate perturbations of brain connections in current augmentation strategies can distort essential structural semantics in the resulting graph views, leading to unrealistic and less explainable representations. This distortion ultimately undermines the effectiveness of SSL-based methods in downstream clinical and diagnostic applications.

To address this issue, we propose SAM-BG, a framework designed for low-supervision settings that uses structure-aware augmentation via edge masking to learn robust, biologically meaningful brain graph representations from large-scale, unlabeled fMRI data. It follows a two-stage learning strategy: (i) *Structure Semantic Extraction*, which pre-trains an edge masker using a small set of labeled data to identify the most discriminative substructures, guided by the information bottleneck (IB) principle [28]. (ii) *SSL with Structure-semantic Preservation*, where the trained edge masker is applied to unlabeled brain graphs to retain key substructures while introducing controlled perturbations to the remaining graph. This ensures that augmented views preserve critical semantic information while adding sufficient variability. Through this design, SAM-BG improves both representation robustness and interpretability, offering insights into disorder-relevant connectivity patterns. Our main contributions are:

- We propose a novel two-stage learning framework, SAM-BG, which improves data efficiency for psychiatric disorder diagnosis by leveraging limited supervision to learn structurally meaningful representations from large-scale, unlabeled brain networks.
- We introduce a learnable masker that enhances the learning of biologically meaningful structural semantics, which in turn improves data augmentation for more effective representation learning in psychological applications.
- Extensive experiments on two real-world fMRI datasets demonstrate that SAM-BG outperforms state-of-the-art methods in low-data scenarios and reveals disorder-specific brain connectivity patterns.

2 Related Work

2.1 Brain Network Analysis on fMRI Data

The fMRI data captures brain connectivity through BOLD signal fluctuations and is widely used in brain network analysis. Traditional methods [16, 20] typically flatten this data into feature vectors, ignoring the brain’s topological structure, an essential aspect for detecting connectivity disruptions in neurological disorders. Graph learning addresses this limitation by representing fMRI data as graphs. BrainGB [4] provides a unified benchmark framework for evaluating graph learning methods on brain networks. Other models, such as BrainGNN [11], employ region-aware pooling to identify key regions of interest (ROIs), thereby enhancing disease-related interpretability. In contrast, IBGNN [5] highlights important ROIs and connections through a learnable global mask. However, these methods heavily depend on labeled data, which is often limited in psychiatric research. To address this challenge, we propose SAM-BG that improves representation learning from unlabeled fMRI data by preserving structural-semantic information during SSL.

2.2 Self-supervised Brain Network Representation Learning

SSL has recently emerged as a powerful approach for learning representations without relying on labeled data, effectively addressing data scarcity [13]. Through data augmentation strategies, SSL enables the extraction of discriminative features. In graph-based SSL, methods like GraphCL [27] generate positive pairs through edge perturbation, node dropping, and subgraph sampling. For brain networks, A-GCL [31] and SF-GCL [18] adopt Bernoulli masking for edge-level perturbations, while BraGCL [14] improves interpretability by incorporating node and edge importance. GCDA [23] further introduces a diffusion-based pretext task to enhance semantic augmentation. However, many existing methods neglect structural semantics during augmentation, leading to biased representations. To overcome this, we propose a structure-aware graph augmentation strategy that generates biologically meaningful views for learning more robust and explainable representations.

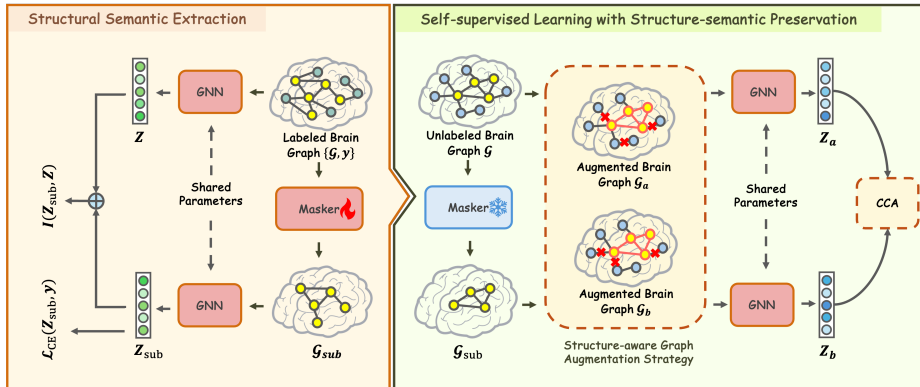


Fig. 1: Overview of the SAM-BG model consisting of structural semantic extraction and SSL with structure-semantic preservation phases.

3 The Proposed Method

The overall framework of SAM-BG is shown in Figure 1. It consists of two main phases: (i) Structural semantic extraction, where an edge masker is trained to identify substructures containing task-relevant structural semantics; (ii) SSL with structure-semantic preservation, where augmentations are applied only to non-salient edges while retaining the extracted substructures, thus enhancing representation learning by maintaining critical structural semantics.

3.1 Structural Semantic Extraction

We represent a brain network as $\mathcal{G} = (\mathcal{V}, \mathcal{E}, \mathbf{A}, \mathbf{X})$, where $\mathcal{V} = \{v_1, v_2, \dots, v_N\}$ denotes N ROIs, $\mathbf{A} \in \mathbb{R}^{N \times N}$ is the adjacency matrix computed via Pearson correlation [21], and $\mathbf{X} \in \mathbb{R}^{N \times D}$ is the node feature matrix with each row \mathbf{x}_i representing the feature vector of ROI v_i . An edge $e_{i,j}$ exists if $a_{i,j}$ indicates significant functional connectivity. Since functional connections are critical for diagnosing psychiatric disorders [7], we introduce an edge masker to extract discriminative substructures from \mathbf{A} as structural prior knowledge.

Specifically, the masker consists of a multi-layer perceptron (MLP) with sigmoid activation, which encodes the upper triangular part of \mathbf{A} to generate a probabilistic edge-selection matrix $\mathbf{P} \in [0, 1]^{N \times N}$, mirrored to preserve symmetry. To enable discrete but differentiable edge sampling, Gumbel-Softmax reparameterization [15] is applied to binarize \mathbf{P} into $\mathbf{P}_{\text{edge}} \in \{0, 1\}^{N \times N}$. The final subgraph is then obtained by masking the original adjacency as $\mathbf{A}_{\text{sub}} = \mathbf{A} \odot \mathbf{P}_{\text{edge}}$. Then, the masker is trained under the Information Bottleneck (IB) principle [28], as illustrated in Figure 1 (left), aiming to retain label-relevant semantics while discarding redundant topology. Specifically, the objective is to minimize the mutual information (MI) between \mathcal{G}_{sub} and \mathcal{G} to encourage compression, while maximizing the MI between \mathcal{G}_{sub} and the label y to ensure discriminability. The objective is formally expressed as:

$$\min_{\mathcal{G}_{\text{sub}}} \beta I(\mathcal{G}_{\text{sub}}, \mathcal{G}) - I(\mathcal{G}_{\text{sub}}, y), \quad (1)$$

where β is the hyperparameters, and $I(\cdot, \cdot)$ is the MI estimation. To compute the first term, we encode the embeddings of \mathcal{G}_{sub} and \mathcal{G} using a shared GNN encoder as \mathbf{Z}_{sub} and \mathbf{Z} . We then use the matrix-based Rényi’s α -order MI estimator [29] to obtain their MI as $I(\mathcal{G}_{\text{sub}}, \mathcal{G}) := I(\mathbf{Z}_{\text{sub}}, \mathbf{Z})$. For the second term, we follow previous work [28] that minimizes the cross-entropy loss between the \mathbf{Z}_{sub} and its ground truth label y as $-I(\mathcal{G}_{\text{sub}}, y) := \mathcal{L}_{\text{CE}}(\mathbf{Z}_{\text{sub}}, y)$. Thus, the final objective becomes:

$$\mathcal{L}_{\text{pre}} = \beta I(\mathbf{Z}_{\text{sub}}, \mathbf{Z}) + \mathcal{L}_{\text{CE}}(\mathbf{Z}_{\text{sub}}, y). \quad (2)$$

This formulation encourages the edge masker to extract compact, label-relevant substructures \mathcal{G}_{sub} that preserve essential structural semantics, performing as the structural prior knowledge.

3.2 Self-supervised Learning with Structure-semantic Preservation

As shown in Figure 1 (right), we propose a representation learning module consisting of a structure-aware graph augmentation strategy with a tailored learning objective to learn semantically meaningful representations for data-efficient diagnosis of psychiatric disorders.

Structure-aware Graph Augmentation Strategy. An effective data augmentation strategy should increase diversity while preserving semantic consistency. To achieve this, we leverage a trained edge masker to transfer structural priors from limited labeled data to large-scale unlabeled data, thereby generating biologically plausible augmented brain graphs that support effective representation learning. Specifically, the masker identifies salient substructures \mathcal{G}_{sub} from an unlabeled graph \mathcal{G} . Augmentation is then performed by introducing controlled perturbations into the complementary non-salient region $\Delta\mathcal{G} = \mathcal{G} \setminus \mathcal{G}_{\text{sub}}$, where edges are randomly removed under a uniform distribution. This process yields two structure-aware augmented views, \mathcal{G}_a and \mathcal{G}_b , which preserve essential semantic structures while ensuring sufficient diversity.

Structure-aware Representation Learning Objective. To capture shared structural semantics across views, SAM-BG employs canonical correlation analysis (CCA) [3] as the core learning objective. Specifically, the two augmented graphs, \mathcal{G}_a and \mathcal{G}_b , are passed through a shared GNN encoder, which is initialized from the pre-training phase. The encoder outputs view-specific embeddings \mathbf{Z}_a and \mathbf{Z}_b , which are aligned in the latent space by maximizing their correlation via a CCA-based loss. The learning objective is defined as:

$$\mathcal{L}_{\text{CCA}} = \|\mathbf{Z}_a - \mathbf{Z}_b\|_{\text{F}}^2 + \lambda \left(\|\mathbf{Z}_a^{\top} \mathbf{Z}_a - \mathbf{I}\|_{\text{F}}^2 + \|\mathbf{Z}_b^{\top} \mathbf{Z}_b - \mathbf{I}\|_{\text{F}}^2 \right), \quad (3)$$

where the λ is the trade-off coefficient, and \mathbf{I} is an identity matrix. The first term of the objective aligns the embeddings of the two augmented graphs in a shared

latent space, promoting perturbation-invariant representations. The second term enforces decorrelation across embedding dimensions, preserving view-specific features and preventing representation collapse.

During inference, unlabeled brain graphs \mathcal{G} are first processed by the pre-trained edge masker to retain key substructures. These structure-aware augmented graphs are then passed through the trained GNN encoder to generate consistent representations for downstream psychiatric disorder classification, ensuring interpretable and clinically relevant features from unlabeled data.

4 Experiment

4.1 Experiment Setup

Datasets. We conducted experiments on two publicly available medical imaging datasets: ABIDE ¹ and ADHD-200 ². Both contain resting-state fMRI data commonly used in psychiatric research. For ABIDE, we used 743 subjects, 364 with autism spectrum disorder (ASD) and 379 healthy controls (HC), aged 6–64, with balanced age and gender distribution. For ADHD-200, we selected 459 participants, including 230 with ADHD and 229 typically developing (TD) individuals, aged 7–21. Brain networks were constructed using the Automated Anatomical Labeling (AAL) atlas, which defines 116 regions of interest ROIs as nodes. Pearson correlation was used to compute edges between ROI time series, resulting in weighted brain graphs.

Baselines. We compare SAM-BG with several representative baselines, including both supervised and SSL methods. For supervised learning, we use BrainGNN [11], which applies ROI-aware pooling, BrainGB [4], and a standardized benchmark. For SSL, we include GraphCL [27], GCA [32], MA-GCL [8], and CCA-SSG [30], which differ in their augmentation and view generation strategies. We adopt the official settings for BrainGNN and BrainGB. All SSL baselines use their original implementations with edge perturbation and 20% labeled data for fine-tuning, simulating low-supervision scenarios.

Implementation Details. Our model is implemented using PyTorch and trained on an NVIDIA Tesla P100 GPU. During pre-training, we leverage 20% of the labeled data to guide masker training. For downstream tasks, the dataset is split into 80% for fine-tuning, 10% for validation, and 10% for testing, with the test set strictly excluded from any supervised training during pre-training. The hyperparameters are configured as follows: the MI trade-off coefficient β is set to 0.01 for ABIDE and 0.001 for ADHD, while the weight of the decorrelation loss term λ is set to $1e^{-4}$ for ABIDE and 0.001 for ADHD. We conduct 5-fold cross-validation and repeat experiments five times with different random seeds. Results are reported as mean and standard deviation of accuracy (ACC), the area under the ROC curve (AUC), recall, and F1-score.

¹ https://fcon_1000.projects.nitrc.org/indi/abide/

² https://fcon_1000.projects.nitrc.org/indi/adhd200/

Table 1: Performance (%) on the ABIDE and ADHD datasets. SL represents supervised learning, and SSL represents self-supervised learning. The best results are bold, and the second results are underlined.

	Methods	ABIDE				ADHD			
		ACC	AUC	Recall	F1-score	ACC	AUC	Recall	F1-score
SL	BrainGNN	54.9 ± 8.7	57.1 ± 8.3	55.0 ± 6.3	53.4 ± 6.0	55.8 ± 1.2	58.0 ± 4.9	46.3 ± 4.2	55.9 ± 4.2
	BrainGB	55.6 ± 4.3	56.3 ± 3.6	55.4 ± 5.2	53.6 ± 10.2	56.2 ± 7.1	59.6 ± 5.2	56.2 ± 4.6	61.6 ± 6.3
SSL	MA-GCL	49.1 ± 7.1	44.8 ± 9.2	52.5 ± 7.6	42.5 ± 11.8	50.1 ± 5.6	48.5 ± 6.2	46.5 ± 3.7	45.2 ± 6.4
	GraphCL	51.3 ± 4.6	50.4 ± 5.7	52.4 ± 7.5	50.3 ± 6.4	51.5 ± 6.8	47.6 ± 5.9	47.8 ± 7.5	46.5 ± 5.6
	GCA	52.8 ± 3.5	50.6 ± 2.4	53.2 ± 4.4	52.1 ± 2.3	50.8 ± 2.4	52.4 ± 5.1	59.4 ± 3.6	53.6 ± 4.4
	CCA-SSG	55.0 ± 6.1	57.2 ± 6.0	55.2 ± 7.7	53.3 ± 6.7	56.6 ± 5.8	60.3 ± 2.6	60.3 ± 4.4	58.0 ± 8.6
	BraGCL	53.5 ± 4.3	55.1 ± 5.2	53.4 ± 4.4	51.8 ± 5.0	63.8 ± 5.6	67.3 ± 3.7	63.8 ± 5.6	63.7 ± 5.5
	A-GCL	59.0 ± 1.6	63.3 ± 1.8	71.6 ± 12.9	<u>63.0 ± 4.1</u>	<u>64.4 ± 2.5</u>	69.0 ± 3.2	<u>68.5 ± 17.2</u>	<u>64.7 ± 3.9</u>
SAM-BG (ours)		63.1 ± 3.4	66.7 ± 4.3	<u>65.9 ± 4.2</u>	66.7 ± 5.2	67.7 ± 3.7	66.5 ± 4.6	68.8 ± 3.8	68.4 ± 5.4

Table 2: Performance (%) of the ablation study for substructure evaluation on the ABIDE and ADHD datasets.

Methods	ABIDE				ADHD			
	ACC	AUC	Recall	F1-score	ACC	AUC	Recall	F1-score
SAM-BG(sub)	50.1 ± 4.3	51.4 ± 5.2	55.6 ± 3.9	51.8 ± 5.5	51.3 ± 3.4	52.5 ± 6.2	53.3 ± 5.6	52.9 ± 5.1
SAM-BG(rest)	46.4 ± 4.5	44.7 ± 4.3	48.1 ± 5.1	44.7 ± 4.8	48.3 ± 4.8	53.7 ± 5.1	49.5 ± 3.2	50.9 ± 6.2
SAM-BG(only)	58.3 ± 5.6	61.3 ± 4.6	57.8 ± 5.7	58.5 ± 7.3	61.3 ± 4.3	60.2 ± 4.2	61.5 ± 7.4	59.5 ± 6.5

4.2 Experimental Results and Discussion

Comprasion Results. Table 1 shows the comparison between our method and baselines on the ABIDE and ADHD datasets. Overall, supervised methods generally outperform most SSL baselines, highlighting the value of label information in graph classification. BrainGB achieves the highest F1-score among supervised methods, showing strong performance under full supervision. Among SSL methods, CCA-SSG performs well due to its non-contrastive design, which better preserves structural-semantic features. Our method, SAM-BG, consistently outperforms all baselines on both datasets. On ABIDE, it improves ACC by 4.1%, AUC by 3.4%, and F1-score by 3.7% compared to the best baseline, although its recall is slightly lower than A-GCL. On ADHD, it achieves 3.3% higher ACC, 0.3% higher recall, and 3.7% higher F1-score, with a marginally lower AUC than A-GCL. Notably, SAM-BG demonstrates more substantial improvements on the ABIDE dataset. This may indicate that disease-related connectivity patterns are more discriminative in the brain networks of individuals with autism, and that SAM-BG’s two-stage training strategy effectively captures these structural and semantic features to deliver superior results.

Ablation Study. In this section, we evaluate the effectiveness of the structure-aware strategy and the semantic quality of extracted substructures, demonstrating our model’s overall robustness and reliability.

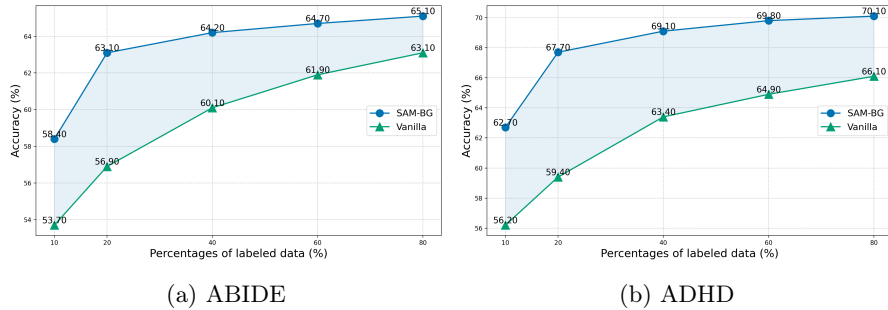


Fig. 2: Comparison between SAM-BG and Vanilla model with the increasing number of labeled data.

The Effectiveness of Extracted Substructure From Masker. To evaluate the role of the identified substructures, we compare three variants: (i) perturbing only the selected substructures (SAM-BG(sub)), (ii) removing them and perturbing the rest of the graph (SAM-BG(rest)), and (iii) using only the substructures for classification (SAM-BG(only)). As shown in Table 2, SAM-BG(rest) performs worst when the substructures are removed, while SAM-BG(only) is closest to the original model. This observation indicates that the identified substructures encode the brain network’s most discriminative and label-relevant semantic features. Disrupting these substructures shifts the model’s attention toward semantically irrelevant structural information, degrading learned representations and impairing downstream performance. These findings empirically validate the effectiveness of our structural masker in isolating non-essential components and preserving core topological semantics. Moreover, they highlight the potential of our method to guide the model toward learning biologically meaningful and task-relevant representations.

The Effectiveness of Structure-aware SSL in Data-efficient Settings. To evaluate the impact of the learnable edge masking strategy in our augmentation process, we compared our model to a vanilla baseline that uses random structural perturbations under varying proportions of labeled data. As shown in Figure 2, our approach consistently outperforms the baseline on both datasets, with accuracy improving as the amount of labeled data increases. Notably, with 20% labeled data, our model achieves the highest gains over the baseline, with improvements of 6.2% and 8.3%, respectively, and delivers performance comparable to the vanilla model trained with 80% labeled data. Furthermore, the results highlight the superior performance of our method in low-label scenarios, where it outperforms most existing SSL approaches even with only 10% labeled data. These findings validate the effectiveness of incorporating structural-semantic priors into the representation learning process. They also highlight the model’s ability to deliver reliable performance even under limited supervision.

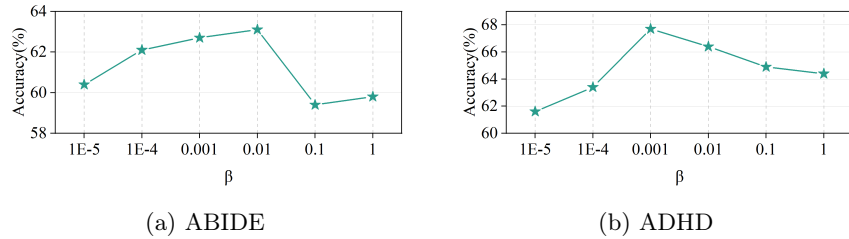


Fig. 3: Accuracy (%) of SAM-BG with different values of β in Equation 2.

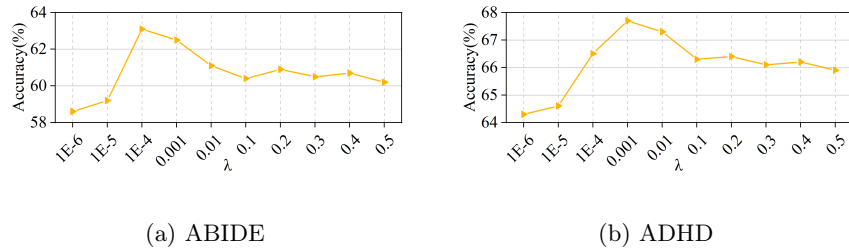


Fig. 4: Accuracy (%) of SAM-BG with different values of λ in Equation 3.

Hyperparameter Tuning Study. We conduct a sensitivity analysis on two key hyperparameters: β and λ . First, β controls the sparsity regularization during the masker pre-training phase. We vary β in the range $[1e^{-5}, 1.0]$ and evaluate its impact on classification performance for ABIDE and ADHD. As shown in Figure 3, small values of β result in weak regularization, leading to substructures with redundant or noisy edges. Conversely, large β values over-prune the graph, potentially removing important connections. A balanced choice of $\beta = 0.01$ for ABIDE and $\beta = 0.001$ for ADHD achieves stable and high accuracy. Second, we examine λ , which weights the decorrelation constraint during representation learning to promote semantic diversity between augmented views. As illustrated in Figure 4, a small λ fails to prevent feature collapse, while a large λ over-emphasizes diversity, impairing invariance learning. Optimal performance is achieved with $\lambda = 1e^{-4}$ for ABIDE and $\lambda = 0.001$ for ADHD, balancing diversity and consistency across views.

Model Explainability Analysis. The edge masker in SAM-BG improves representation learning and interpretability by identifying discriminative substructures that reflect abnormal brain connectivity patterns in psychiatric disorders. To demonstrate this, Figure 5 visualizes the top 20 connections from patients' adjacency matrices, with nodes color-coded by nine functional networks and edge thickness indicating connection strength. In the ABIDE dataset, our method identified increased internal connectivity within the VN and enhanced connectivity between the LIN and other networks, including the DMN and FPN, reflecting heightened sensory sensitivity and over-processing of emotional inputs

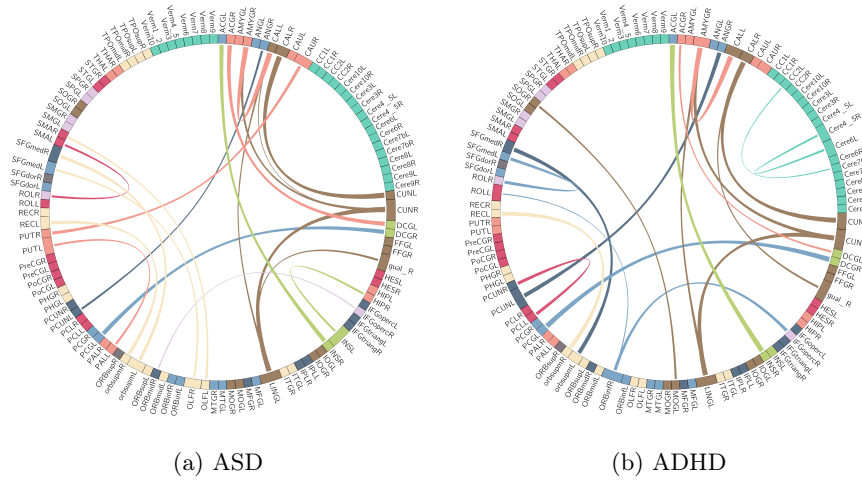


Fig. 5: Explainable graph connections in brain networks of patients with ASD and ADHD. The colors of brain networks are described as visual network (VN), somatomotor network (SMN), dorsal attention network (DAN), ventral attention network (VAN), limbic network (LIN), frontoparietal network (FPN), default mode network (DMN), cerebellum (CBL) and subcortical network (SBN), respectively.

in autism [1,6]. In the ADHD dataset, the model highlights hyperconnectivity in the VAN, particularly in the right hemisphere, along with elevated internal connectivity within the CBL. These patterns are consistent with evidence linking the cerebellum to attention control and the VAN to stimulus-driven attention, supporting their relevance in ADHD [12]. Interestingly, both datasets show increased VN connectivity, suggesting a shared neural signature that may underlie their frequent comorbidity. These results demonstrate that SAM-BG can uncover meaningful, explainable connectivity patterns, offering improved diagnostic insights into psychiatric disorders.

5 Conclusion

We propose SAM-BG, a novel framework that leverages structural priors to enable biologically meaningful brain graph representation learning under limited supervision. SAM-BG first trains an edge masker on a small labeled subset to extract salient connections, capturing key structural semantics. It then generates structure-aware augmentations by perturbing only non-essential edges, preserving semantic integrity for robust SSL. Experiments show that SAM-BG significantly improves psychiatric disorder detection in low-data settings and offers interpretable insights into brain connectivity, highlighting its potential for real-world neuroscience applications.

References

1. Abbott, A.E., Linke, A.C., Nair, A., Jahedi, A., Alba, L.A., Keown, C.L., Fishman, I., Müller, R.A.: Repetitive behaviors in autism are linked to imbalance of corticostriatal connectivity: a functional connectivity mri study. *Social Cognitive and Affective Neuroscience* **13**(1), 32–42 (2018)
2. Amemiya, S., Takao, H., Abe, O.: Resting-state fmri: Emerging concepts for future clinical application. *Journal of Magnetic Resonance Imaging* **59**(4), 1135–1148 (2024)
3. Andrew, G., Arora, R., Bilmes, J., Livescu, K.: Deep canonical correlation analysis. In: *International Conference on Machine Learning*. pp. 1247–1255. PMLR (2013)
4. Cui, H., Dai, W., Zhu, Y., Kan, X., Gu, A.A.C., Lukemire, J., Zhan, L., He, L., Guo, Y., Yang, C.: Braingb: A benchmark for brain network analysis with graph neural networks. *IEEE Transactions on Medical Imaging* **42**(2), 493–506 (2022)
5. Cui, H., Dai, W., Zhu, Y., Li, X., He, L., Yang, C.: Interpretable graph neural networks for connectome-based brain disorder analysis. In: *International Conference on Medical Image Computing and Computer-Assisted Intervention*. pp. 375–385. Springer (2022)
6. Eggebrecht, A.T., Elison, J.T., Feczko, E., Todorov, A., Wolff, J.J., Kandala, S., Adams, C.M., Snyder, A.Z., Lewis, J.D., Estes, A.M., et al.: Joint attention and brain functional connectivity in infants and toddlers. *Cerebral Cortex* **27**(3), 1709–1720 (2017)
7. Gallo, S., El-Gazzar, A., Zhutovsky, P., Thomas, R.M., Javaheripour, N., Li, M., Bartova, L., Bathula, D., Dannlowski, U., Davey, C., et al.: Functional connectivity signatures of major depressive disorder: machine learning analysis of two multicenter neuroimaging studies. *Molecular Psychiatry* **28**(7), 3013–3022 (2023)
8. Gong, X., Yang, C., Shi, C.: Ma-gcl: Model augmentation tricks for graph contrastive learning. In: *Proceedings of the AAAI Conference on Artificial Intelligence*. vol. 37, pp. 4284–4292 (2023)
9. Hyman, S.L., Levy, S.E., Myers, S.M., Kuo, D., Apkon, S., Brei, T., Davidson, L.F., Davis, B.E., Ellerbeck, K.A., Noritz, G.H., et al.: Executive summary: identification, evaluation, and management of children with autism spectrum disorder. *Pediatrics* **145**(1) (2020)
10. Li, Q., Seraji, M., Calhoun, V.D., Iraj, A.: Complexity measures of psychotic brain activity in the fmri signal. In: *2024 IEEE Southwest Symposium on Image Analysis and Interpretation (SSIAI)*. pp. 9–12. IEEE (2024)
11. Li, X., Zhou, Y., Dvornek, N., Zhang, M., Gao, S., Zhuang, J., Scheinost, D., Staib, L.H., Ventola, P., Duncan, J.S.: Braingnn: Interpretable brain graph neural network for fmri analysis. *Medical Image Analysis* **74**, 102233 (2021)
12. Lin, H., Lin, Q., Li, H., Wang, M., Chen, H., Liang, Y., Bu, X., Wang, W., Yi, Y., Zhao, Y., et al.: Functional connectivity of attention-related networks in drug-naive children with adhd. *Journal of attention disorders* **25**(3), 377–388 (2021)
13. Liu, Y., Jin, M., Pan, S., Zhou, C., Zheng, Y., Xia, F., Philip, S.Y.: Graph self-supervised learning: A survey. *IEEE Transactions on Knowledge and Data Engineering* **35**(6), 5879–5900 (2022)
14. Luo, X., Dong, G., Wu, J., Beheshti, A., Yang, J., Xue, S.: An interpretable brain graph contrastive learning framework for brain disorder analysis. In: *Conference on Web Search and Data Mining (WSDM’24)* (2024)
15. Maddison, C., Mnih, A., Teh, Y.: The concrete distribution: A continuous relaxation of discrete random variables. In: *Proceedings of the International Conference*

- on Learning Representations. International Conference on Learning Representations (2017)
16. Pan, X., Xu, Y.: A novel and safe two-stage screening method for support vector machine. *IEEE Transactions on Neural Networks and Learning Systems* **30**(8), 2263–2274 (2018)
 17. Peng, C., He, J., Xia, F.: Learning on multimodal graphs: A survey. *ArXiv Preprint ArXiv:2402.05322* (2024)
 18. Peng, C., Liu, M., Meng, C., Xue, S., Keogh, K., Xia, F.: Stage-aware brain graph learning for alzheimer’s disease. *MedRxiv pp. 2024–04* (2024)
 19. Peng, C., Liu, M., Meng, C., Yu, S., Xia, F.: Adaptive brain network augmentation based on group-aware graph learning. In: *The Second Tiny Papers Track at ICLR 2024* (2024)
 20. Plitt, M., Barnes, K.A., Martin, A.: Functional connectivity classification of autism identifies highly predictive brain features but falls short of biomarker standards. *NeuroImage: Clinical* **7**, 359–366 (2015)
 21. Schober, P., Boer, C., Schwarte, L.A.: Correlation coefficients: appropriate use and interpretation. *Anesthesia & Analgesia* **126**(5), 1763–1768 (2018)
 22. Sun, K., Peng, C., Yu, S., Han, Z., Xia, F.: From eeg data to brain networks: Graph learning based brain disease diagnosis. *IEEE Intelligent Systems pp. 1–9* (2024). <https://doi.org/10.1109/MIS.2024.3352972>
 23. Wang, X., Fang, Y., Wang, Q., Yap, P.T., Zhu, H., Liu, M.: Self-supervised graph contrastive learning with diffusion augmentation for functional mri analysis and brain disorder detection. *Medical Image Analysis* **101**, 103403 (2025)
 24. Xia, F., Peng, C., Ren, J., Febrinanto, F.G., Luo, R., Saikrishna, V., Yu, S., Kong, X.: Graph learning. *arXiv preprint arXiv:2507.05636* (2025)
 25. Xie, Y., Xu, Z., Zhang, J., Wang, Z., Ji, S.: Self-supervised learning of graph neural networks: A unified review. *IEEE Transactions on Pattern Analysis and Machine Intelligence* **45**(2), 2412–2429 (2022)
 26. Yang, J., Gohel, S., Vachha, B.: Current methods and new directions in resting state fmri. *Clinical Imaging* **65**, 47–53 (2020)
 27. You, Y., Chen, T., Sui, Y., Chen, T., Wang, Z., Shen, Y.: Graph contrastive learning with augmentations. *Advances in Neural Information Processing Systems* **33**, 5812–5823 (2020)
 28. Yu, J., Xu, T., Rong, Y., Bian, Y., Huang, J., He, R.: Recognizing predictive substructures with subgraph information bottleneck. *IEEE Transactions on Pattern Analysis and Machine Intelligence* **46**(3), 1650–1663 (2021)
 29. Yu, S., Giraldo, L.G.S., Jenssen, R., Principe, J.C.: Multivariate extension of matrix-based rényi’s α -order entropy functional. *IEEE Transactions on Pattern Analysis and Machine Intelligence* **42**(11), 2960–2966 (2019)
 30. Zhang, H., Wu, Q., Yan, J., Wipf, D., Yu, P.S.: From canonical correlation analysis to self-supervised graph neural networks. *Advances in Neural Information Processing Systems* **34**, 76–89 (2021)
 31. Zhang, S., Chen, X., Shen, X., Ren, B., Yu, Z., Yang, H., Jiang, X., Shen, D., Zhou, Y., Zhang, X.Y.: A-gcl: Adversarial graph contrastive learning for fmri analysis to diagnose neurodevelopmental disorders. *Medical Image Analysis* **90**, 102932 (2023)
 32. Zhu, Y., Xu, Y., Yu, F., Liu, Q., Wu, S., Wang, L.: Graph contrastive learning with adaptive augmentation. In: *Proceedings of the Web Conference 2021. pp. 2069–2080* (2021)